

## Numerical Analysis on the Effect of Parameters that Affect the Flow Rate through the Tunnel with Jet Fan Ventilation System

Sa Ryang Kim<sup>†</sup>, Nahmkeon Hur<sup>\*</sup>, Youngil Kim<sup>\*\*</sup>, Ki-Jung Kim<sup>\*\*\*</sup>

*Department of Precision Mechanical Engineering, Kangnung National University, Gangneung 210-702, Korea*

*<sup>\*</sup>Department of Mechanical Engineering, Sogang University, Seoul 121-742, Korea*

*<sup>\*\*</sup>Thermal/Flow Control Research Center, KIST, Seoul 136-791, Korea*

*<sup>\*\*\*</sup>Graduate School, Sogang University, Seoul 121-742, Korea*

**Key words:** Tunnel, Jet fan, Ventilation, Pressure rise, Friction factor, CFD, Roughness height, Swirl angle, Hub/tip ratio

**ABSTRACT:** In this study, ventilation flow rate and pressure rise through a tunnel are simulated numerically using computational fluid dynamics (CFD) for various conditions such as roughness height of the surface of tunnel, swirl angle and hub/tip ratio of jet fan, and entrance and exit effects. By using a modified wall function, friction factor can be predicted with respect to the Moody chart within 10% of error for the circular pipe flow and 15% for the present tunnel. For more accurate design, the effect of the swirl angle and hub/tip ratio of jet fan, which is not included in the theoretical equation of pressure rise by jet fan needs to be considered.

### Nomenclature

<hr style="border: 0.5px solid black; margin-bottom: 5px;"/> <p><math>A_j</math> : exit area of jet fan [m<sup>2</sup>]  <math>A_m</math> : equivalent frontal area of vehicle [m<sup>2</sup>]  <math>A_r</math> : cross sectional area of tunnel [m<sup>2</sup>]  <math>C_\mu</math> : coefficient in equation of turbulence model, 0.09  <math>D</math> : displacement thickness [m]  <math>D_f</math> : diameter of jet fan, 1.25 [m]  <math>D_r</math> : diameter of tunnel, 8.69 [m]  <math>k</math> : turbulent kinetic energy [m<sup>2</sup>/s<sup>2</sup>]  <math>M</math> : number of vehicles  <math>N</math> : number of jet fan  <math>\Delta P_j</math> : pressure rise by a jet fan [Pa]  <math>\Delta P_m</math> : pressure rise by vehicles [Pa]  <math>\Delta P_{MTW}</math> : pressure loss by natural wind [Pa]</p> <hr style="border: 0.5px solid black; margin-top: 5px;"/>	<p><math>\Delta P_r</math> : pressure loss by friction of tunnel wall [Pa]  <math>Q_j</math> : exit flow rate of jet fan [m<sup>3</sup>/s]  <math>R_{hub}/R_{tip}</math> : hub/tip ratio of jet fan  <math>U_j</math> : exit velocity of jet fan [m/s]  <math>U_n</math> : wind velocity [m/s]  <math>U_r</math> : air velocity in tunnel [m/s]  <math>u^+</math> : non-dimensionalized velocity at wall, <math>(u - u_{wall})/u_\tau</math>  <math>u_\tau</math> : wall friction velocity [m/s]  <math>V_t</math> : velocity of vehicle [m/s]  <math>y^+</math> : non-dimensionalized distance from wall, <math>\rho C_\mu^{1/4} k^{1/2} y/\mu</math>  <math>y_0</math> : roughness height [m]</p> <p style="text-align: center;"><b>Greek symbols</b></p> <p><math>\lambda_r</math> : friction coefficient of tunnel  <math>\kappa</math> : von Karman constant, 0.42  <math>\mu</math> : viscosity [kg/(m·s)]</p>
--	--

<sup>†</sup> Corresponding author

Tel.: +82-33-640-2395; fax: +82-33-640-2244

E-mail address: dearksr@kangnung.ac.kr



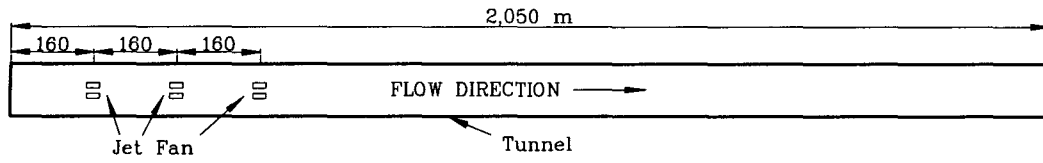


Fig. 2 Planar view of tunnel and installed jet fans by pair.

schematics of the cross-section and the planar section of the tunnel.

In the present study, the effect of the roughness height of the wall, the swirl angle of jet fan, hub/tip ratio ( $R_{hub}/R_{tip}$ ) of jet fan, 2.5 m/s of wind at the tunnel exit, and existence of computational region before the entrance and after the exit of the tunnel on the ventilation flow rate through the tunnel is examined. Table 1 shows the values of parameters and boundary conditions for each simulation case.

To consider the effect of wall roughness height, the modified logarithmic wall function,<sup>(7)</sup> Eqn. (1) is used.

$$u^+ = A + \frac{1}{\kappa} \log \frac{y^+ - D^+}{B + CR^+} \quad (1)$$

where,  $D^+ = \rho C_\mu^{1/4} k^{1/2} D / \mu$ ,  $R^+ = \rho C_\mu^{1/4} k^{1/2} y_0 / \mu$ , and  $A$ ,  $B$  and  $C$  are constants. Total of 10 cases were examined with different roughness height,  $y_0$ , which varied from 0 to 40 mm.

Jet fan was modeled to be a solid cylinder with two inlet boundaries with uniform velocity for both inlet and exit of jet fans. The exit

flow rate of jet fans was fixed for all case.

Simulations were performed for two swirl angles, 17° and 30°, which had been used in the experiment of Martegani et al.<sup>(1)</sup> The rotating direction of jet fan has also been considered. The cases of co-rotating fans (S1F, S2F) and counter-rotating fans (S1, S2) were simulated and compared. As for the boundary condition at the inlet and exit of jet fan, the circumferential velocity was added so that the resultant velocity vector had the same angle with the swirl angle to the axis of rotation.

For the effect of hub/tip ratio, simulations were carried out for two cases, where  $R_{hub}/R_{tip} = 0.18$  and 0.40, which had also been examined by Martegani et al.<sup>(1)</sup>(Fig. 3).

The wind velocity outside the tunnel exit was assumed to be 2.5 m/s of which value is generally accepted in the road tunnel design. The effect of wind was considered by applying given pressure boundary condition at the tunnel exit. The effect of the wind outside the tunnel was modeled with 2 cases and the results were compared with each other. One (B1) was that the wind flows backward through the tunnel

Table 1 Simulation cases for tunnel ventilation with jet fans

Case	Roughness height										Swirl angle				Hub/tip ratio		Exit condition		Entrance loss	Exit loss		
	R1	R2	R3	R4	R5	R6	R7	R8	R9	R10	S1	S1F	S2	S2F	H1	H2	B1	B2	E1	E2		
Roughness height (mm)	0	1	2	5	10	20	30	35	37	40	37				37		37		37	37		
Swirl angle	0°										17°		30°		0°		0°		0°		0°	0°
$R_{hub}/R_{tip}$	0										0				0.18 0.40		0		0		0	0
Exit B.C.	P <sub>atm</sub>										P <sub>atm</sub>				P <sub>atm</sub>		$\Delta P_{MTW}$   $\frac{\rho U_n^2}{2}$		P <sub>atm</sub>	P <sub>atm</sub> at far field		
Entrance B.C.	P <sub>atm</sub>										P <sub>atm</sub>				P <sub>atm</sub>		P <sub>atm</sub>		P <sub>atm</sub> at far field	P <sub>atm</sub>		

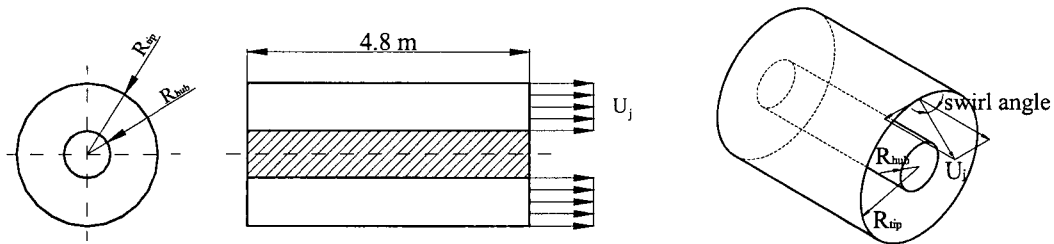


Fig. 3 Definition of hub and tip radius, and swirl angle.

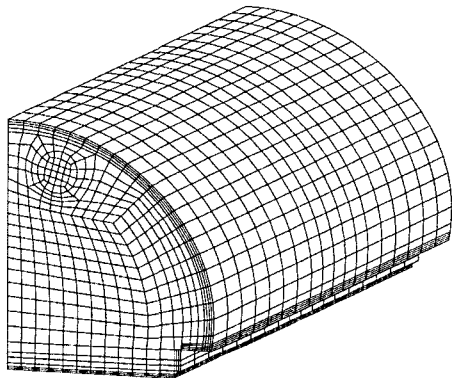


Fig. 4 Part of meshes for tunnel with jet fan.

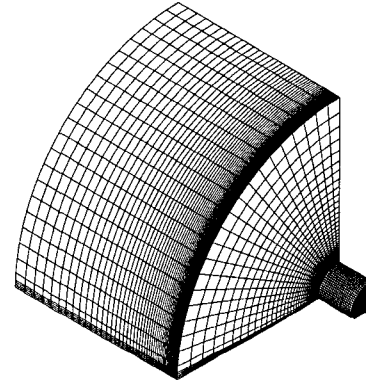


Fig. 5 Meshes for entrance of tunnel.

from the exit to the entrance with a velocity of 2.5 m/s, and the other (B2) was that the pressure at the exit is equivalent to a dynamic pressure of 2.5 m/s.

The computational domain for the entrance and exit regions were considered to examine the effect of the position of the surface where boundary condition is given.

Because the geometry of tunnel is symmetric with respect to the center plane, the mesh was generated only for the half of the tunnel. The number of meshes for the inside of tunnel was about 390,000, and for the entrance region about 90,000. A enlarged part of meshes for the inside of tunnel is shown in Fig. 4, and that of the entrance region in Fig. 5. For calculation, STAR-CD<sup>(7)</sup> V3.1 was used on a Linux Cluster (Dual Pentium III 850 Mhz CPU, 7 node, 512 MB RAM/node). Each case was calculated using one CPU, which took about 7 days for each case. Mesh density test was performed with doubled mesh, and the difference of the flow rates ob-

tained was less than 2%. Therefore, for all simulation cases, the mesh of 390,000 was used. For examining the effect of rotational direction of the jet fan, simulations were carried out with the mesh including the full tunnel geometry (S1F, S2F), since symmetry along the center line can no longer be applied.

### 3. Results and discussion

The role of the jet fans is to generate the ventilating flow through the tunnel. The ventilating flow is governed by the momentum of jet and the pressure recovered at downstream. The distribution of pressure along the tunnel was shown in Fig. 6. The pressure rise by jet fans was obtained by the pressure difference at the intersection of vertical axis and the line (dotted line in the figure) that has been extrapolated from the linear pressure distribution downstream of the jet.<sup>(8)</sup> The ventilation flow rate was calculated by integrating the velocity

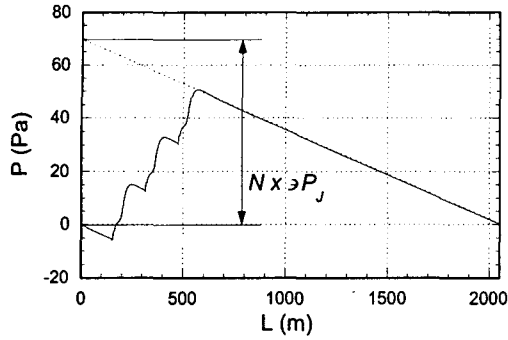


Fig. 6 Pressure distribution along the center of the tunnel.

multiplied by area at each cell. Friction factor was obtained from the gradient of the linear part of pressure distribution.

To examine the result of the numerical simulation, the calculated ventilation flow rates were compared with the values from design equations. The analytical equations<sup>(9)</sup> to calculate the design values are as follows.

$$\Delta P_{MTW} + \Delta P_r - \Delta P_m \leq N \times \Delta P_j \quad (2)$$

where,  $\Delta P_{MTW}$  is pressure rise by wind outside the tunnel,  $\Delta P_r$  is pressure loss by friction on the tunnel wall,  $\Delta P_m$  is pressure rise by traffics,  $\Delta P_j$  is pressure rise by a jet fan, and each term is as follows.

$$\Delta P_{MTW} = \left(1 + \zeta_e + \lambda_r \frac{L_r}{D_r}\right) \frac{\rho}{2} U_n^2 \quad (3)$$

$$\Delta P_r = \left(1 + \zeta_e + \lambda_r \frac{L_r}{D_r}\right) \frac{\rho}{2} U_r^2 \quad (4)$$

$$\Delta P_m = \frac{A_m}{A_r} \frac{\rho}{2} M (V_i - U_r)^2 \quad (5)$$

$$\Delta P_j = \rho Q_j (U_j - U_r) \eta_1 \eta_2 \eta_3 \frac{1}{A_r} \quad (6)$$

The pressure rise by traffic vehicles was not considered in the present study, so the corresponding term was neglected when the design flow rate was calculated using the equation. By inserting each term (3), (4) and (6) into Eqn. (2), it becomes a quadratic equation with respect to the mean velocity of the tunnel,  $U_r$ .

Table 2 Results of ventilation flow rate, friction factor, pressure rise

		Roughness height (mm)									
Case		R1	R2	R3	R4	R5	R6	R7	R8	R9	R10
Values		0	1	2	5	10	20	30	35	37	40
Relative roughness		0	0.000115	0.000230	0.000575	0.00115	0.00230	0.00345	0.00403	0.00423	0.00460
Flowrate (cms)	CFD	546	487	459	421	390	360	342	335	332	330
	Design	301									
Friction factor	CFD	0.00896	0.0113	0.0130	0.0156	0.0180	0.0214	0.0237	0.0247	0.0251	0.0256
	Design	0.025									
Pressure rise by a jet fan (Pa)	CFD	11.1	11.2	11.3	11.4	11.5	11.5	11.5	11.5	11.5	11.6
	Eq. (6)	9.63	9.96	10.1	10.3	10.5	10.7	10.8	10.8	10.8	10.8
	Design	11.0									
		Swirl angle				Hub/tip ratio		Exit condition		Entrance region	Exit region
Case		S1	S1F	S2	S2F	H1	H2	B1	B2	E1	E2
Values		17°		30°		0.18	0.40	-	-	-	-
Flowrate (cms)	CFD	328	326	317	315	338	363	267	320	297	332
	Design	301				301		234		290	301
Friction factor	CFD	0.0251	0.0249	0.0251	0.0247	0.0251	0.0251	0.0261	0.0261	0.0251	0.0251
	Design	0.025									
Pressure rise by a jet fan (Pa)	CFD	11.2	11.0	10.4	10.2	12.0	13.8	12.4	11.7	11.9	11.6
	Eq. (6)	10.9	10.9	10.9	10.9	11.5	15.5	11.2	10.9	11.0	10.8
	Design	11.0				11.0		11.4		11.0	11.0

The ventilation flow rate was then calculated from the mean velocity multiplied by the cross sectional area of the tunnel.

Table 2 shows the ventilation flow rate, friction factor, pressure rise by a jet fan for all cases by numerical simulation and design values.

### 3.1 Examination of modified wall function

To examine the applicability of the modified wall function Eqn. (1) to the present study, the circular pipe flows were simulated for the Reynolds number of  $2 \times 10^6$ , which was similar to that of the present tunnel. The relation of friction factor with respect to the roughness height of wall was compared with the Moody chart<sup>(10)</sup> and Colebrook's equation.<sup>(10)</sup> The results are shown in Fig. 7. The simulation predicted about 10% lower values compared with that of the Moody chart and Colebrook's equation. Since the trends are in good agreement, the modified wall function at the tunnel wall has been used for all simulations in this study.

### 3.2 Ventilation flow rate and friction factor

The variation of the ventilation flow rate and the friction factor for the roughness height of the tunnel wall is shown in Fig. 8. The ventilation flow rate calculated by the design Eqn.

(2) was about  $301 \text{ m}^3/\text{s}$  when the friction factor was 0.025. For a smooth wall, the numerical prediction of the ventilation flow rate was 80% larger than the design equation. For a roughness height of 37 mm (relative roughness of 0.043), the friction factor becomes 0.0251 which is close to 0.025, the value used in the design equation. Then the error of the ventilation flow rate is reduced to 10%. Therefore, it is found that the consideration of the roughness of the wall is important and should be included in the numerical simulation.

The friction factor was predicted about 15% lower than that from Moody chart. The error was larger than the circular pipe flow, because the shape of the cross section of the tunnel was not circular and the flow was eccentric. Thus, the numerical simulation with appropriate consideration of the roughness of the tunnel wall can predict the ventilation flow rate and friction factor through the tunnel within 10 ~ 15% error. In the present study, since the roughness of the tunnel wall was not well known, all the simulations were performed assuming the roughness height of the wall as 37 mm of which value predicted the closest friction factor used in the design.

Figure 9 shows the result for the swirl angle. If the jet fans rotates opposite relative to each other, the symmetric assumption becomes valid.

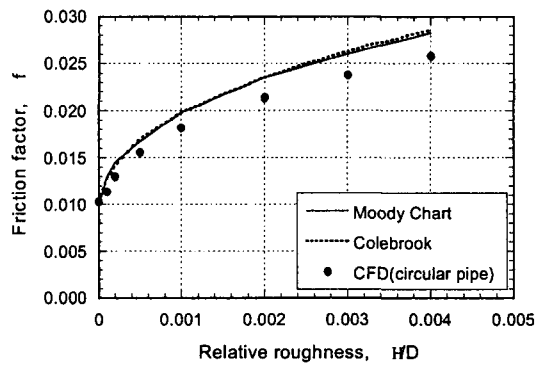


Fig. 7 Comparison of friction factor with CFD and conventional data ( $Re_D = 2 \times 10^6$ ).

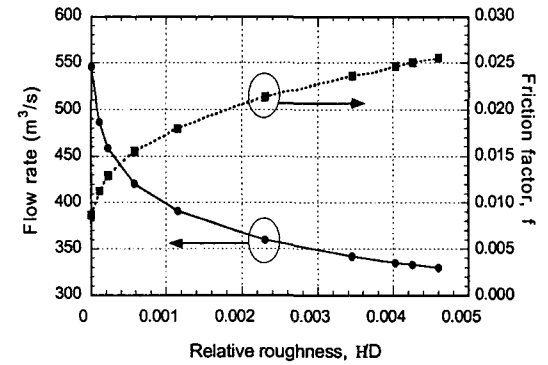


Fig. 8 Comparison of flow rates and friction factors of the tunnel for various relative roughness.

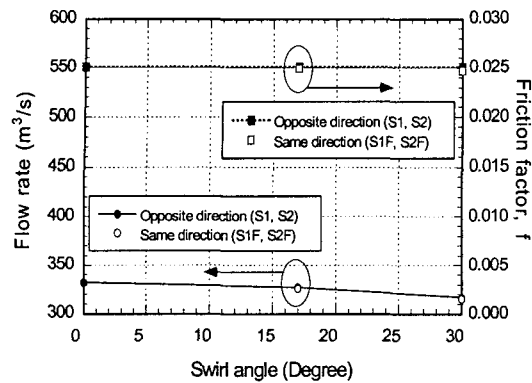


Fig. 9 Comparison of flow rate and friction factor for various swirl angle.

But, in most cases the rotational direction of fans will be the same, so the flow field will not be symmetric and the full tunnel geometry should be included in the simulation domain. In Table 1, S1 and S2 are symmetric cases while S1F and S2F are not. As the swirl angle increased, the friction factor did not vary while the ventilation flow rate decreased about 5%. It was because the circumferential velocity component made the secondary flow active and raised the total loss through the tunnel. The rotational direction of jet fan did not affect the friction factor nor the ventilation flow rate, because the two jet fans were located so sufficiently far apart not to cause any interaction. Hence, to determine the effect of swirl, further study on the parameters such as the distance

between the fans and the distance from the wall are necessary, and these effects should be considered in the design equation.

Figure 10 shows the results for considering hub/tip ratio. As the hub/tip ratio increased, the effective flow area of jet decreased and the exit velocity of jet fan increased. So, it was expected that the induced flow rate by jet fan increased and total flow rate through tunnel increased. The simulation result showed that the friction factor did not vary but the flow rate increased up to 10% as the hub/tip ratio increased. Though the hub is short and the velocity distribution would not be uniform in the actual jet fan unlike the trend depicted in Fig.3, the result showed that the exit velocity of jet fan had significant effect on the ventilation flow rate through the tunnel. Therefore, it is important to consider the appropriate boundary condition for the jet fan.

Figure 11 shows the simulation results for a wind of 2.5 m/s outside the tunnel exit. Due to the exit resistance, the ventilation flow rate decreased about 5~20%, while the friction factor increased a little. In this case, the results of numerical simulation showed over 15% error compared with the design value. In the figure, case B1 considered all the terms of Eqn. (3), which means that 2.5 m/s wind blew backward through the tunnel. But in actual situation, where the fans are operating and vehicles moving,

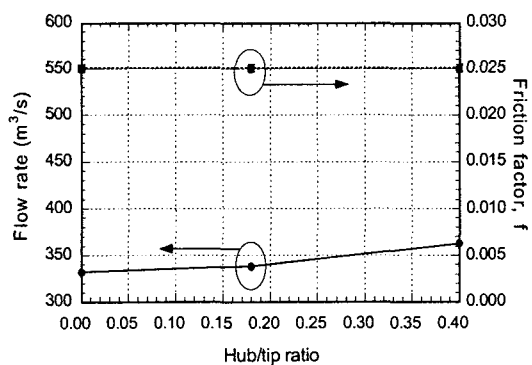


Fig. 10 Ventilation flow rate and friction factor for different hub/tip radius ratio.

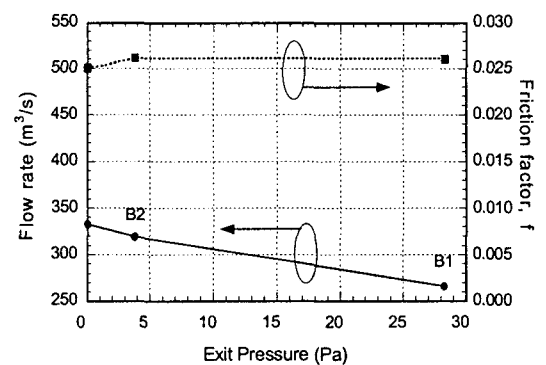


Fig. 11 Ventilation flow rate and friction factor for different backward flow.

this would not happen. Therefore, for the back flow wind at the exit as in case B2, it is more appropriate to consider only the first term in Eqn. (3) assuming that it acts as a pressure resistance of which value is equivalent to the dynamic pressure of the wind. The present design equation gives somewhat excessive ventilation flow rate. Therefore, to predict the ventilation flow rate accurately in the numerical simulation, further study is necessary for the boundary condition of the wind outside the tunnel.

By considering the entrance region, the ventilation flow rate was similar with the design value (Table 2) though most other cases predicted over about 10% larger values. This was because the loss at the entrance was predicted greater than that of the design equation. Hence, the consideration of the appropriate entrance geometry and loss coefficient was necessary to get more precise results for the numerical simulation. As the length of the tunnel is increased, the ratio of the entrance loss to the total loss is decreased. Since the entrance loss was about 10% of total in the present tunnel, further study on the effect of entrance shape is recommended.

The existence of the exit region did not affect the ventilation flow rate nor the friction factor (Table 2). Therefore, it is sufficient to apply the exit boundary condition directly at the exit of the tunnel.

### **3.3 Pressure rise by jet fans**

To obtain the number of jet fan for tunnel ventilation, it is necessary to calculate exactly not only the required pressure rise of the left hand side of Eqn. (6), but also the pressure rise due to a jet fan in the right hand side. Different pressure rises were compared and shown in Table 2 which are obtained by calculating the pressure gradient along the length of the tunnel from the result of numerical sim-

ulation (Fig. 6), by inserting the flow rate from the result of numerical simulation into Eqn. (6), and from theoretical design equation Eqn. (2).

The pressure rise with respect to the variation of the roughness of the wall did not show much difference between different methods of calculation. The pressure rise calculated by Eqn. (6) with the ventilation flow rate from the result of numerical simulation was smaller than that of other methods because the numerical simulation predicted greater ventilation flow rate.

As the swirl angle increased, the pressure rise obtained from the pressure distribution decreased, but that from the ventilation flow rate did not vary. The reason is that the effect of the swirl angle on the pressure rise is not included in the Eqn. (6).

When hub/tip ratio was considered, the effect of the increase of exit velocity of jet fan was larger than that of the increase of the flow rate on the equation, which makes the prediction of the pressure rise greater than the design value.

By considering the wind outside the tunnel exit, the error varied about 10% depending on the boundary condition.

Since the ventilation flow rate of the simulation which considers the entrance region was similar to the design value, the pressure rise calculated from the design equation agrees well with the design value, but differs from the value obtained from the pressure distribution through the tunnel. The existence of exit region has negligible effect on the result.

Therefore, to predict the pressure rise accurately, it would be necessary to study the effect of various parameters on the jet fan and include those effects in the design equation. And it is also necessary to examine the method for calculating the pressure rise from the result of numerical simulation.



#### 4. Conclusions

In the present study, the effect of various parameters that affect the flow rate of tunnel with jet fan ventilation was examined by numerical simulation, and the conclusions are as follows.

(1) By using the modified logarithmic wall function, the friction factor at tunnel wall can be estimated with an error of less than 10% in the circular pipe flow and 15% in the present tunnel flow.

(2) With the same wall friction factor, the simulated flow rate was predicted about 10% larger than the designed value. Therefore, it is necessary to consider the wall roughness in numerical simulation to obtain reasonable flow rate and friction factor.

(3) The entrance region should be included in the simulation domain to consider entrance effect. The predicted pressure loss due to entrance in the simulation was larger than that of the design equation. Therefore, further study is necessary to find the relation between the entrance shape of tunnel and the pressure loss.

(4) Two methods for considering the effect of 2.5 m/s wind outside the tunnel exit resulted in largely different flow rates. So further study on the appropriate boundary condition for the wind outside the tunnel exit seems necessary.

(5) The rotating direction of the fans did not affect the flow rate. The distance between the fans seemed to be sufficient so that the interaction had no effects. But in general, the full geometry should be modeled to consider the rotational direction of fans.

(6) The swirl angle and the hub/tip ratio affected the flow rate through the tunnel. But these parameters might depend on the designer or the manufacturer of the fan. Therefore, the correct boundary condition for the fan should be applied for more precise prediction of the characteristics in the flow through the tunnel.

(7) In addition to the known parameters for

the fan installation efficiency, additional parameters, such as the swirl angle of the exit velocity and the hub/tip ratio of fan should be considered to get more accurate flow rate and pressure rise through the tunnel.

#### References

1. Martegani, A. D., Pavesi, G. and Barbetta, C., 2000, Experimental investigation of interaction of plain jet fans mounted in series, 10th International Symposium on Aerodynamics and Ventilation of Vehicle Tunnel, BHR Group, pp. 1055-1078.
2. Saika, T., Nakajima, K. and Setoyama, S., 2000, Jet fan thrust performance evaluation installed in road tunnel, 10th International Symposium on Aerodynamics and Ventilation of Vehicle Tunnel, BHR Group, pp. 1079-1088.
3. Hur, N., 1999, Ventilation simulation in the long rail tunnel of Young-dong line, Report of Dae-Yang Air Conditioning Co. Ltd., SGI-19997012, Industrial Technology Research Center, Sogang Univ.
4. Mizuno, A., Nakajima, K. and Kanoh, T., 1999, Study on the installation interval of jet fans for road tunnel ventilation, Proceedings of Sixth STAR-CD Users' Seminar, CD-Adapco-Japan, pp. 13-15.
5. Lim, J.-S. and Shin, D.-S., 2001, Numerical simulation of fluid field around a road tunnel, Proceedings of the SAREK Summer Annual Conference, pp. 1079-1083.
6. Yang, P.-S., Cho, Y.-J. and Lee, J.-H., 1998, A study on the ventilation in a long road tunnel, KSME J. (B), Vol. 22, No. 8, pp. 1091-1100.
7. STAR-CD Version 3.1 Manual, 1999, Computational Dynamics Limited.
8. Diaz, J., Kramesberge, F. and Gaehler, 1991, Optimized jet fan installation, 7th International Symposium on Aerodynamics and Ventilation of Vehicle Tunnel, BHR Group,

- Brington, UK, pp. 821-826.
9. Technology of Tunnel Ventilation, 2000, Bumchang Engineering, pp. 62-76.
10. Cho, K. R., Yoo, J. Y. and Kang, S. H. (Translated), 2000, Fluid Mechanics, 4th ed., McGraw-Hill Korea, pp. 350-351.